Effective apparent diffusion coefficient parameters for differentiation between mass-forming autoimmune pancreatitis and pancreatic ductal adenocarcinoma

Hainan Ren[1] · Naoko Mori[1] · Shin Hamada[2] · Chiaki Takasawa[1] · Shunji Mugikura[1] · Atsushi Masamune[2] · Kei Takase[1]

Abstract

Purpose To evaluate the diagnostic performance of apparent diffusion coefficient (ADC) parameters by region of interest (ROI) methods in differentiating mass-forming autoimmune pancreatitis (AIP) from pancreatic ductal adenocarcinoma (PDAC).

Methods The institutional review board approved this retrospective study and the requirement for informed consent was waived. Twenty-three patients with mass-forming AIP and 144 patients with PDAC underwent diffusion-weighted imaging with b-values of 0 s/mm^2 and 800 s/mm^2. The minimum, maximum, and mean ADC values obtained by placing ROIs within lesions and percentile ADC values (10th, 25th, 50th, 75th, and 90th) from entire-lesion histogram analysis were compared between the two groups by using Mann–Whitney U tests. The diagnostic performance was evaluated by receiver operating characteristic (ROC) curve analysis.

Results The minimum, maximum, and mean ADC values were significantly different between mass-forming AIP and PDAC groups. ROC curve analysis showed that the maximum ADC had the highest diagnostic performance (0.92), while the minimum ADC value had the lowest diagnostic performance (0.72). The AUC of minimum ADC was significantly lower than that of maximum or mean ADC ($P < 0.0001$, $P < 0.0001$). The AUC was lowest in 10th percentile ADC value and highest in 90th percentile value. The AUC increased along with the increase of percentile values.

Conclusion Either the maximum or mean ADC value was effective in differentiating mass-forming AIP from the PDAC group, while the minimum ADC value might not be recommended.

Keywords Mass-forming autoimmune pancreatitis · Pancreatic ductal adenocarcinoma · Apparent diffusion coefficient · Diffusion-weighted imaging · Magnetic resonance imaging

Abbreviations

AIP	Autoimmune pancreatitis
MRCP	Magnetic resonance cholangiopancreatography
PDAC	Pancreatic ductal adenocarcinoma
ADC	Apparent diffusion coefficient
ROI	Region of interest

✉ Naoko Mori
naokomori7127@gmail.com

Hainan Ren
renhainan1994@gmail.com

Shin Hamada
oep.tdgf1@gmail.com

Chiaki Takasawa
chiaki.tak@gmail.com

Shunji Mugikura
mugi844@gmail.com

Atsushi Masamune
amasamune@med.tohoku.ac.jp

Kei Takase
ktakase@rad.med.tohoku.ac.jp

[1] Department of Diagnostic Radiology, Tohoku University Graduate School of Medicine, 1-1 Seiryo-machi, Aoba-ku, Sendai 980-8574, Japan

[2] Division of Gastroenterology, Tohoku University Graduate School of Medicine, Sendai, Japan

Introduction

Autoimmune pancreatitis (AIP) is histologically characterized by an autoimmune inflammatory process in which dense T lymphocytes and IgG4-positive plasma cells with prominent fibrosis in the interlobular and peripancreatic area of the pancreas are observed [1, 2]. The representative magnetic resonance (MR) imaging features of AIP are low signal intensity on T1-weighted images, a capsule-like rim with low signal intensity on T2-weighted images, irregular narrowing of the main pancreatic duct on magnetic resonance cholangiopancreatography (MRCP), and homogeneous enhancement on the delayed phase of dynamic contrast-enhanced (DCE) MR images [3–5].

AIP is generally classified into two types: diffuse type characterized by diffuse enlargement of the pancreas and mass-forming type characterized by segmental/focal enlargement of the pancreas [4–6]. Mass-forming AIP sometimes shares similar radiological features with pancreatic ductal adenocarcinoma (PDAC). Single or multiple lesions with low signal intensity on T1-weighted images and upstream dilatation of the main pancreatic duct on MRCP are observed in both mass-forming AIP and PDAC [7–11]. To avoid unnecessary pancreatic resections in patients with mass-forming AIP, accurate imaging methods to differentiate mass-forming AIP from PDAC are needed [12].

Currently, diffusion-weighted (DW) imaging is used to characterize pancreatic abnormalities [7, 8, 13–15]. Quantitative apparent diffusion coefficient (ADC) values calculated from the signal intensity on DW images reflect the degree of diffusivity of water molecules [13]. In previous studies, region of interest (ROI) methods were performed to obtain ADC values. The mean ADC value obtained by placing as large ROIs as possible within lesions was used to differentiate mass-forming AIP from PDAC [7, 8, 14, 15]. In other areas such as breast tumors, several studies found that the minimum ADC value by placing multiple small ROIs within lesions was significantly different between malignant and benign tumors or different grades of breast cancer [16, 17]. In brain astrocytic tumors, Murakami et al. reported that maximum ADC value by placing multiple small ROIs within lesions was significantly different among tumor grades [18]. Histologically, the minimum ADC value is considered to reflect tumor cellularity [19], while the maximum ADC might reflect the lowest cellular zone composed of stroma. Furthermore, the presence of intratumoral anaplasia, such as fibrosis and necrosis, and mucin production, might affect ADC values, especially maximum ADC values [16, 20, 21]. To our knowledge, no study has evaluated the diagnostic performance of the minimum and maximum ADC values by ROI methods in differentiating mass-forming AIP from PDAC. Placing small or large ROIs on ADC maps by human eyes to evaluate the minimum, maximum, and mean ADC values might be subjective. A pixel-based entire-lesion histogram analysis could obtain percentile ADC values objectively, which can help verify the ADC values by ROI methods [22, 23].

The purpose of our study was to evaluate the diagnostic performance of ADC parameters by ROI methods in differentiating mass-forming AIP from PDAC.

Materials and methods

Patients

The institutional review board approved this retrospective study and waived the requirement for informed consent. Consecutive patients who underwent initial MRI examination using the same machine and the same scanning protocol with a contrast agent between April 2008 and August 2020 were enrolled. For the mass-forming AIP group, 249 patients were selected using the search term "autoimmune pancreatitis." Among them, 166 patients who met the revised version of the Japan Pancreas Society (JPS) 2018 diagnostic criteria were included [4, 5]. (a) Patients diagnosed as diffuse-type AIP ($n = 131$), (b) those diagnosed with other cancers owing to the difficulty of ruling out the possibility of pancreatic metastases ($n = 8$), and (c) those in whom DW imaging was not performed ($n = 4$) were excluded from the study. A total of 23 patients with mass-forming AIP were enrolled. According to the JPS 2018 diagnostic criteria, the final diagnosis of 22 patients was made based on the histological findings of endoscopic ultrasound-guided fine-needle aspiration (EUS-FNA). One patient was diagnosed by the combination of irregular narrowing of the main pancreatic duct on MRCP, elevated serum IgG4 level ($\geqq 135$ mg/dL), and presence of extra-pancreatic lesions (lacrimal glands). For the PDAC group, 294 patients were selected using the search terms "pancreatic cancer" or "pancreatic adenocarcinoma" from our radiological database. Among them, 151 patients with histological diagnosis of PDAC using EUS-FNA ($n = 100$) or surgery ($n = 51$) were included. Seven patients in whom DW imaging was not performed were excluded from the PDAC group. Finally, 144 patients with PDAC were enrolled in this study. The median time interval between MRI examination and histological diagnosis of PDAC was 10 days (range 0–75 days).

MRI examination protocol

All patients underwent MRI examination of the abdomen using a 3.0 T system (MAGNETOM Trio, A Tim System,

Siemens Healthcare GmbH, Erlangen, Germany). The patients were imaged in the supine position with 12 coil elements. The pancreatic MRI protocols at our hospital included the following sequences: a T1-weighted two-dimensional (2D) dual gradient-recalled echo sequence (2000/126 [repetition time (TR) in milliseconds/echo time (TE) in milliseconds] with fat saturation; field of view, 320 mm × 380 mm; acquisition matrix, 147 × 256; section thickness, 7 mm; acquisition time, 17 s), a breath-hold multi-shot T2-weighted sequence (TR 2450 ms/TE 102 ms with fat saturation; field of view, 320 mm × 380 mm; acquisition matrix, 179 × 320; section thickness, 7 mm; acquisition time, 29 seconds). Respiratory-triggered DW imaging was performed with single-shot echo planar imaging with motion-probing gradients in three directions (TR 1000 ms/TE 65 ms; field of view, 380 mm; acquisition matrix, 90 × 128; section thickness, 7 mm; acquisition time, 18 seconds; application of motion-probing gradient pulse along the *x*, *y*, and *z* directions; number of excitations, 2). ADC maps were automatically created with *b*-values of 0 s/mm^2 and 800 s/mm^2. DCE-MR imaging scans were performed using a three-dimensional (3D) fat-suppressed T1-weighted 3D turbo field-echo sequence to obtain arterial (30–35 s), portal (65–70 s), delayed (3 min) and hepatobiliary (15 min) phases after the injection of gadoxetate disodium (0.025 mmol/kg). The contrast agent was injected as a rapid bolus and immediately followed by 30–35 mL of saline flush through a power injector at a rate of 2 mL/s.

Image analysis

Two experienced radiologists (*N.M and **C.T with ***11 and ****9 years of experience in radiology of the abdomen, respectively) reviewed all MR images blinded to the radiological diagnosis and clinical and histological results on a commercially available workstation (HMC Viewer Ver. V1.0.0, Hitachi, Japan). The location of lesions (head, uncinate, body and tail) and sizes (the maximum diameter) were evaluated using the portal phase of the DCE-MR images.

ADC values by ROI methods

All ROIs were placed independently by the two radiologists. There are various histological components such as solid component, fibrosis, mucin and necrosis in PDAC. To detect heterogeneity within lesions, we placed multiple ROIs both in solid component and non-solid component of the lesions. Three oval or round ROIs were placed where the ADCs visually appeared to be lowest within the tumor contour on ADC maps to measure the average ADC values of the individual ROIs: the minimum of these was the minimum ADC (Fig. 1a, b, and c). Similarly, three ROIs were placed where the ADCs visually appeared to

be highest within the tumor contour to measure the average ADC values of the individual ROIs: the maximum of these was the maximum ADC (Fig. 1a–c). The difference between maximum and minimum ADCs was recorded as the difference ADC.

To obtain mean ADC values, three oval or round ROIs that covered as much of the lesion as possible were placed on ADC maps (Fig. 1d, e, and f). When the contour of a lesion was too blurry to discriminate, ROIs were placed so as not to include the contour. When there were fewer than three lesion slices, one or two ROIs were placed. Subsequently, the final mean ADC value was calculated by averaging the ADC values obtained from the ROIs. Care was taken to avoid the main pancreatic duct, pancreatic vessels, and artifacts.

All ROIs for the minimum, maximum, and mean ADC values occupied at least three pixels (> 36 mm^2).

Percentile ADC values from a pixel-based entire-lesion histogram analysis

For histogram analysis, the MRI data from the ADC maps were transferred to a personal computer and processed using the ImageJ software, version 1.47 (http://imagej.nih.gov/ij/). Using the portal phase of DCE-MR images as reference (Fig. 2b), we carefully performed manual segmentation to delineate the entire lesion on each slice of the ADC maps (Fig. 2a). The data acquired from each slice were summed to derive the cumulative frequency distributions with ADC values on the x-axis and the cumulative frequency percentage on the y-axis.

Statistical analysis

The interobserver reliability of the ADC values by ROI methods was assessed using the ICC. *R* values of 1.0, 0.81–0.99, 0.61–0.80, 0.41–0.60, 0.21–0.40, and 0.20 or less indicated perfect agreement, almost perfect agreement, substantial agreement, moderate agreement, fair agreement, and slight agreement, respectively [24]. Mann–Whitney *U* tests were used to compare the minimum, maximum, difference, and mean ADC values by ROI methods and the 10th, 25th, 50th, 75th and 90th percentile ADC values obtained from histogram analysis between the mass-forming AIP and PDAC groups. Receiver operating characteristic (ROC) curve analysis using areas under the curve (AUCs) was used to evaluate the diagnostic performance of the ADC values by ROI methods and percentile ADC values obtained from histogram analysis in differentiating the two groups. The AUCs of the minimum, maximum, and mean ADC values by ROI methods were compared. Statistical analysis was performed using JMP Pro 14 (SAS Institute Inc., Cary, NC, USA). Statistical differences with *p* < 0.05 were considered
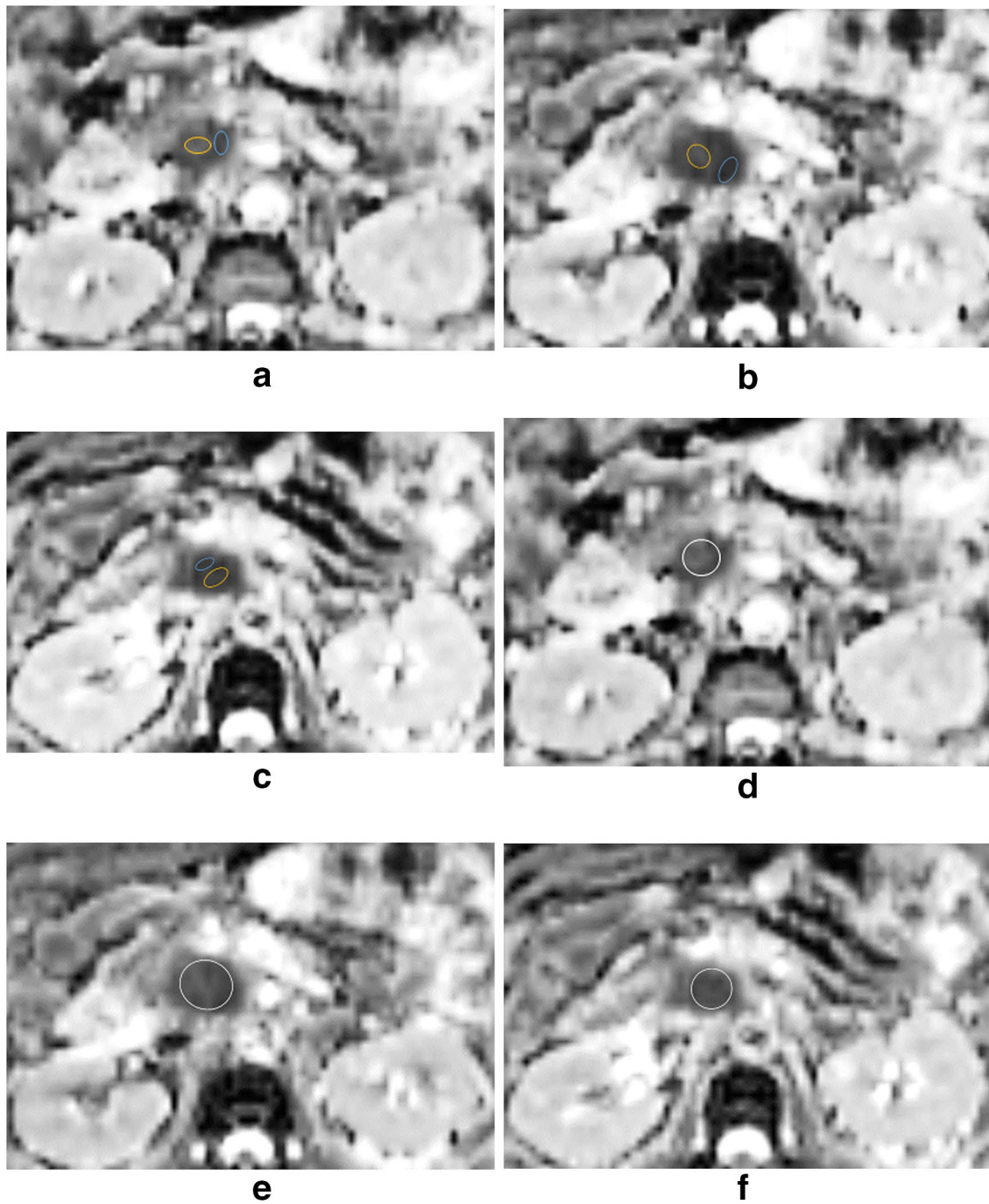
Fig. 1 Magnetic resonance images of a 61-year-old man with biopsy-confirmed pancreatic ductal adenocarcinoma (PDAC). **a–c** Three slices of apparent diffusion coefficient (ADC) maps were shown. Three regions of interest (ROIs) were placed where the ADCs visually appeared to be lowest within the tumor contour on ADC maps to obtain average ADC values of the individual ROIs (blue circles). The minimum of these was recorded as the minimum ADC. In the same manner, three ROIs were placed to obtain maximum ADC (orange circles). In this case, the minimum and maximum ADC values were $0.92 \times 10^{-3} \text{mm}^2/\text{s}$ and $1.81 \times 10^{-3} \text{mm}^2/\text{s}$, respectively. **d–f** Three ROIs covering as much of the lesion as possible were placed to obtain average ADC values (white circles). In this case, the mean ADC value was $1.35 \times 10^{-3} \text{mm}^2/\text{s}$

statistically significant. After the Bonferroni correction of 4 multiple comparisons, the critical value became < 0.012 (0.05/4).

Results

Patient and lesion characteristics are shown in Table 1. In the authors' evaluation of the agreement between two readers, the ICCs for the minimum, maximum, difference and mean ADC values were 0.94, 0.86, 0.79, and 0.94, respectively.

All the ADC parameters by ROI methods were significantly different between the mass-forming AIP and PDAC groups (Table 2). All the percentile ADC values were significantly different between the mass-forming AIP and PDAC groups (Table 3).

In ROC curve analysis, the maximum ADC value showed the highest diagnostic performance (AUC: 0.92), whereas the minimum ADC value showed the lowest diagnostic performance (AUC: 0.72). The AUC of minimum ADC was significantly lower than those of maximum or mean ADC ($p < 0.0001$ and $p < 0.0001$) (Fig. 3). No significant difference was
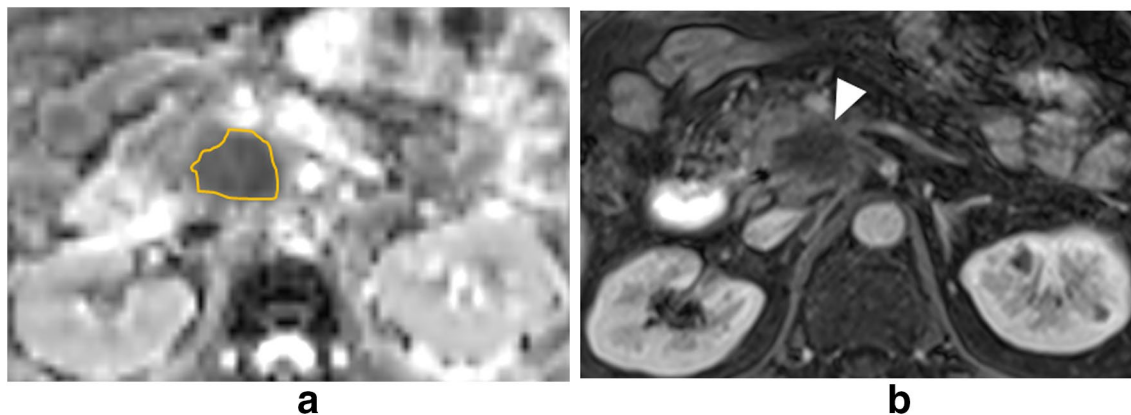

Fig. 2 Segmentation for histogram analysis to obtain percentile apparent diffusion coefficient (ADC) values. Magnetic resonance (MR) images of a 61-year-old man with biopsy-confirmed pancreatic ductal adenocarcinoma (PDAC). Manual segmentation is performed to delineate the whole lesion as much of the lesion volume as possible on each slice of ADC maps (**a**) with reference to the portal phase of dynamic contrast-enhanced (DCE)-MR images (white arrowhead) (**b**)

Table 1 Patient and lesion characteristics of the mass-forming autoimmune pancreatitis (AIP) and pancreatic ductal adenocarcinoma (PDAC) groups

Variables	Mass-forming AIP ($n = 23$)	PDAC ($n = 144$)
Gender (female/male (%))	4 (17%)/19 (83%)	62 (43%)/82 (57%)
Age (years)	64 (47–81)	68 (41–92)
Lesion location		
Head (%)	13 (57%)	50 (35%)
Uncinate (%)	2 (9%)	22 (15%)
Body (%)	3 (13%)	44 (31%)
Tail (%)	5 (21%)	27 (19%)
Size (mean ± SD) (mm)	36 ± 14	34 ± 16

[a]Data are expressed in medians, and the numbers inside the parentheses are the ranges

Table 2 Apparent diffusion coefficient (ADC) parameters by ROI methods in differentiating mass-forming autoimmune pancreatitis (AIP) from pancreatic ductal adenocarcinoma (PDAC)

Variable (10^{-3} mm^2/s)	Mass-forming AIP ($n = 23$)	PDAC ($n = 144$)	P value	AUC
Minimum ADC	0.95 ± 0.18	1.12 ± 0.22	0.0007[a]	0.72
Maximum ADC	1.21 ± 0.26	1.70 ± 0.31	< 0.0001[a]	0.92
Difference ADC	0.26 ± 0.20	0.57 ± 0.31	< 0.0001[a]	0.82
Mean ADC	1.10 ± 0.19	1.40 ± 0.23	< 0.0001[a]	0.88

Data are expressed in mean ± standard deviation

AUC area under receiver operating characteristic (ROC) curve

[a]Statistically significant difference

Table 3 Percentile apparent diffusion coefficient (ADC) values obtained from histogram analysis in differentiating between mass-forming autoimmune pancreatitis (AIP) and pancreatic ductal adenocarcinoma (PDAC)

Variables (10^{-3} mm^2/s)	Mass-forming AIP ($n = 23$)	PDAC ($n = 144$)	P value	AUC
10th percentile	0.96 ± 0.14	1.16 ± 0.22	< 0.0001[a]	0.79
25th percentile	1.03 ± 0.15	1.27 ± 0.22	< 0.0001[a]	0.83
50th percentile	1.12 ± 0.14	1.40 ± 0.24	< 0.0001[a]	0.86
75th percentile	1.24 ± 0.15	1.55 ± 0.25	< 0.0001[a]	0.88
90th percentile	1.39 ± 0.17	1.73 ± 0.27	< 0.0001[a]	0.88

Data are expressed in mean ± standard deviation

AUC area under receiver operating characteristic (ROC) curve

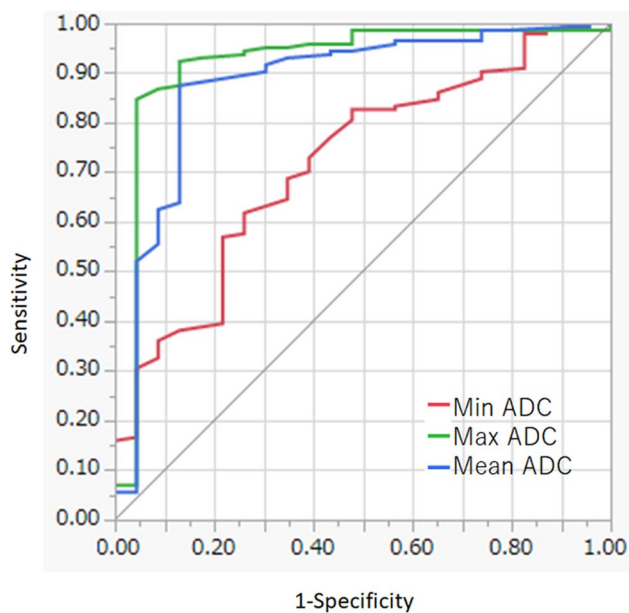[a]Statistically significant difference

Fig. 3 Receiver operating characteristic (ROC) curve analysis to evaluate the diagnostic performance of the apparent diffusion coefficient (ADC) parameters by ROI methods. The AUCs of the minimum, maximum, and mean ADC values are 0.72, 0.92, and 0.88, respectively

found between AUC of maximum ADC and mean ADC ($P =$ 0.074). Difference ADC was significantly different between mass-forming AIP and PDAC; however, AUC of ROC curve analysis was 0.82, which was less than maximum (0.92) and mean ADC (0.88). In histogram analysis, the AUC of ROC curve analysis was lowest in 10th percentile ADC value and highest in 90th percentile value (Table 3). The AUC increased along with the increase of percentile values.

Discussion

The results in this study suggest that the ADC parameters by ROI methods could be helpful in differentiating mass-forming AIP from PDAC with statistical significance. Among these ADC parameters, the diagnostic performance of the maximum and mean ADC values was significantly higher than that of the minimum ADC value. Although selecting the appropriate areas or placing small or large ROIs on ADC maps by human eyes might be subjective, the interobserver reliability of the maximum and mean ADC values was almost perfect in this study.

The mucin and necrosis are considered to be specific histological components in PDAC [25]. The mucin and necrosis resulting from tumor growth are accompanied by more free water molecules, leading to high ADC values [18]. Herneth et al. reported that the areas with high ADC value correlated with histologically areas of mucin and necrosis during tumor progression [20]. To our knowledge, the maximum ADC value has not been used in differentiating mass-forming AIP from PDAC, although the maximum ADC value yielded good diagnostic performance in grading brain astrocytic gliomas and differentiating benign from malignant breast tumors [16–18]. In this study, the maximum ADC value showed the highest diagnostic performance (AUC = 0.92). Based on these findings, the maximum ADC value probably reflecting mucin and necrosis might be a potentially effective parameter in differentiating mass-forming AIP from PDAC.

Histologically, mass-forming AIP contains cellularity and fibrosis [1], while PDAC comprises cellularity, fibrosis, mucin, and necrosis [25, 26]. Therefore, cellularity and fibrosis are histological features found in both mass-forming AIP and PDAC. Decreased ADC values are considered to arise from restricted random motion of water molecules [13]. In this study, the lowest ADC value was recorded as the minimum ADC value, which might correspond to histological cellularity and fibrosis [7]. Since cellularity and fibrosis are common histological features found in mass-forming AIP and PDAC, the minimum ADC value might have the lowest diagnostic performance in differentiating the two groups among ADC parameters by ROI methods. In differentiating benign from malignant abdominal lesions, Feuerlein et al. reported that a number of benign abdominal lesions can exhibit restricted random motion of water molecules or low ADC values, thus mimicking malignant

lesions [27]. The ADC parameter such as the minimum ADC value, corresponding to cellularity and fibrosis, may overlap between benign and malignant abdominal lesions. Our results might be consistent with their findings, and the minimum ADC value might not be recommended.

In our study, the AUC of the mean ADC value was 0.88, and no significant difference was found in the AUCs between the mean and maximum ADC values. Although the mean ADC value from the ROIs that covered as much of the lesion as possible could not detect heterogeneity within the tumor, the mean ADC value with larger ROIs is easy to manage in clinical practice compared with the minimum and maximum ADC values.

We performed pixel-based entire-lesion histogram analysis. Histogram analysis has been used in other areas, such as metastatic ovarian or primary peritoneal cancers, and breast cancer [28, 29]. In pancreatic lesions, Ma et al. reported that the 50th and 100th percentile ADC values could help differentiate mass-forming AIP from PDAC [22]. The maximum ADC value showed the highest diagnostic performance among ADC parameters by ROI methods in our study. Similar to the ADC by ROI methods, the diagnostic performance increased from 10th (0.79) to 90th (0.88) percentile ADC values. Histogram analysis supported that higher ADC values showed better diagnostic performance. Because performing histogram analysis is time-consuming, the maximum and mean ADC values by ROI methods are more acceptable than percentile ADC values obtained from histogram analysis considering their clinical convenience.

This study had several limitations. First, the sample size was small. Second, although the authors carefully tried to avoid the main pancreatic duct, it might be inevitably involved in the placement of ROIs, especially if it has high ADC values, or manual segmentation in histogram analysis. The dilatation of the main pancreatic duct is rarely observed in mass-forming AIP but a relatively common finding in PDAC [12, 30]. If the main pancreatic duct with high ADC values was involved in ROIs in PDAC cases, it might cause increased maximum ADC values, increasing the diagnostic performance of the maximum ADC value in differentiating mass-forming AIP from PDAC. Third, we did not perform point-to-point radiological and histological correlation analysis. We could not perform histological quantification of cellularity, fibrosis, necrosis, and mucin. The location and histological quantification of such components should be compared to areas with lowest and highest ADC values in the future. Fourth, two selective b-values (0 and 800 s/mm^2) were used to measure ADC values in our study. Currently, the effectiveness of parameters from intravoxel incoherent motion diffusion-weighted MR imaging to evaluate pancreatic tumors was reported [31, 32]. Further studies are needed to clarify the most suitable b value for differentiating mass-forming AIP from PDAC. Fifth, there is a potential

population bias in this study. We enrolled mass-forming AIP and PDAC patients with MRI examination using the same machine and the same scanning protocol. In our institution, studies to establish international consensus for the treatment of AIP were performed [33]. Therefore, the ratio between mass-forming AIP and PDAC was uneven in our archive. To reduce the selection bias, further multi-center study would be needed. Sixth, the diagnostic performance of the combination of the ADC parameters by ROI methods and morphological findings including enhancement patterns of the pancreas and upstream dilatation of the main pancreatic duct was not evaluated. To confirm the results of this study, future prospective studies with morphological findings are needed. Nevertheless, this study has several strengths. We clarified that the optimal ADC parameters in differentiating mass-forming AIP from PDAC were the maximum or mean ADC values by ROI methods. The minimum ADC value might not be recommended in differentiating the two groups, although it is used for the evaluation of lesions in other areas such as breast and brain.

In conclusion, either the maximum or mean ADC value was effective in differentiating mass-forming AIP from PDAC, while the minimum ADC value might not be recommended.

Compliance with ethical standards

Conflict of interest The authors have no conflict of interest to disclose.

Ethical approval This study was approved by the Institutional Review Board.

Informed consent Informed consent was waived.

References

1. Finkelberg DL, Brugge WR (2006) Autoimmune Pancreatitis. New England Journal of Medicine 355: 2670-2676. https://org.doi/full/10.1056/NEJMoa0903068

2. Khandelwal A, Inoue D, Takahashi N (2020) Autoimmune pancreatitis: an update. Abdom Radiol 45:1359–1370. https://doi.org/10.1007/s00261-019-02275-x

3. Chari ST (2007) Diagnosis of autoimmune pancreatitis using its five cardinal features: introducing the Mayo Clinic's HISORt criteria. J Gastroenterol 42:39–41. https://doi.org/10.1007/s00535-007-2046-8

4. Shimosegawa T, Chari ST, Frulloni L, et al (2011) International Consensus Diagnostic Criteria for Autoimmune Pancreatitis. 40 (3):352-358. https://doi.org/10.1097/MPA.0b013e3182142fd2

5. The Japan Pancreas Society; The Research Program on Intractable Diseases from the Ministry of Labor and Welfare of Japan. [Japanese clinical diagnostic criteria for autoimmune pancreatitis, 2018 (proposal)—revision of Japanese clinical diagnostic criteria for autoimmune pancreatitis, 2011. J Jpn Pancreas (Suizo) 2018 33:902–913. https://www.jstage.jst.go.jp/article/suizo/33/6/33_902/_pdf/-char/ja

6. Chari ST, Smyrk TC, Levy MJ, et al (2006) Diagnosis of Autoimmune Pancreatitis: The Mayo Clinic Experience. Clinical Gastroenterology and Hepatology 4:1010–1016. https://doi.org/10.1016/j.cgh.2006.05.017

7. Kamisawa T, Takuma K, Anjiki H, et al (2010) Differentiation of Autoimmune Pancreatitis From Pancreatic Cancer by Diffusion-Weighted MRI: American Journal of Gastroenterology 105:1870–1875. https://doi.org/10.1038/ajg.2010.87

8. Takuma K (2012) Strategy to differentiate autoimmune pancreatitis from pancreas cancer. WJG 18 (10):1015-1020. https://doi.org/10.3748/wjg.v18.i10.1015

9. Hoshimoto S, Aiura K, Tanaka M, et al (2016) Mass-forming type 1 autoimmune pancreatitis mimicking pancreatic cancer: Mass-forming autoimmune pancreatitis. Journal of Digestive Diseases 17:202–209. https://doi.org/10.1111/1751-2980.12316

10. Muhi A, Ichikawa T, Motosugi U, et al (2012) Mass-forming autoimmune pancreatitis and pancreatic carcinoma: Differential diagnosis on the basis of computed tomography and magnetic resonance cholangiopancreatography, and diffusion-weighted imaging findings. J Magn Reson Imaging 35:827–836. https://doi.org/10.1002/jmri.22881

11. Working members of Research Committee for Intractable Pancreatic Disease and Japan Pancreas Society, Kawa S, Okazaki K, et al (2010) Japanese consensus guidelines for management of autoimmune pancreatitis: II. Extrapancreatic lesions, differential diagnosis. J Gastroenterol 45:355–369. https://doi.org/10.1007/s00535-009-0197-5

12. Shankar A, Srinivas S, Kalyanasundaram S (2020) Icicle sign: autoimmune pancreatitis. Abdom Radiol 45:245–246. https://doi.org/10.1007/s00261-019-02323-6

13. Barral M, Taouli B, Guiu B, et al (2015) Diffusion-weighted MR Imaging of the Pancreas: Current Status and Recommendations. Radiology 274:45–63. https://doi.org/10.1148/radiol.14130778

14. Choi S-Y, Kim SH, Kang TW, et al (2016) Differentiating Mass-Forming Autoimmune Pancreatitis From Pancreatic Ductal Adenocarcinoma on the Basis of Contrast-Enhanced MRI and DWI Findings. American Journal of Roentgenology 206:291–300. https://doi.org/10.2214/AJR.15.14974

15. Taniguchi T, Kobayashi H, Nishikawa K, et al (2009) Diffusion-weighted magnetic resonance imaging in autoimmune pancreatitis. Jpn J Radiol 27:138–142. https://doi.org/10.1007/s11604-008-0311-2

16. Hirano M, Satake H, Ishigaki S, et al (2012) Diffusion-Weighted Imaging of Breast Masses: Comparison of Diagnostic Performance Using Various Apparent Diffusion Coefficient Parameters. American Journal of Roentgenology 198:717–722. https://doi.org/10.2214/AJR.11.7093

17. Mori N, Ota H, Mugikura S, et al (2013) Detection of invasive components in cases of breast ductal carcinoma in situ on biopsy by using apparent diffusion coefficient MR parameters. European Radiology 23:2705–2712. https://doi.org/10.1007/s00330-013-2902-2

18. Murakami R, Hirai T, Sugahara T, et al (2009) Grading Astrocytic Tumors by Using Apparent Diffusion Coefficient Parameters: Superiority of a One-versus Two-Parameter Pilot Method1. Radiology 251:838–845. https://doi.org/10.1148/radiol.2513080899

19. Sugahara T, Korogi Y, Kochi M, et al (1999) Usefulness of diffusion-weighted MRI with echo-planar technique in the evaluation of cellularity in gliomas. J Magn Reson Imaging 9:53–60. https://doi.org/10.1007/s11604-011-0047-2

20. Herneth AM, Guccione S, Bednarski M (2003) Apparent Diffusion Coefficient: a quantitative parameter for in vivo tumor characterization. European Journal of Radiology 45:208–213. https://doi.org/10.1016/S0720-048X(02)00310-8

21. Lyng H, Haraldseth O, Rofstad EK (2000) Measurement of cell density and necrotic fraction in human melanoma xenografts by diffusion weighted magnetic resonance imaging. Magn Reson Med. 43(6):828-36. https://doi.org/10.1002/1522-2594(200006)43:6%3c828::AID-MRM8%3e3.0.CO;2-P

22. Ma X, Zhao X, Ouyang H, et al (2014) Quantified ADC histogram analysis: a new method for differentiating mass-forming focal pancreatitis from pancreatic cancer. Acta Radiologica 55:785–792. https://doi.org/10.1177/0284185113509264

23. Kang Y, Choi SH, Kim Y-J, et al (2011) Gliomas: Histogram Analysis of Apparent Diffusion Coefficient Maps with Standard- or High-b-Value Diffusion-weighted MR Imaging—Correlation with Tumor Grade. Radiology 261:882–890. https://doi.org/10.1148/radiol.11110686

24. Landis JR, Koch GG (1977) The Measurement of Observer Agreement for Categorical Data. Biometrics 33:159. https://doi.org/10.2307/2529310

25. Yoon SE, Byun JH, Kim KA, et al (2010) Pancreatic ductal adenocarcinoma with intratumoral cystic lesions on MRI: correlation with histopathological findings. BJR 83:318–326. https://doi.org/10.1259/bjr/69770140

26. Sugiyama Y, Fujinaga Y, Kadoya M, et al (2012) Characteristic magnetic resonance features of focal autoimmune pancreatitis useful for differentiation from pancreatic cancer. Jpn J Radiol 30:296–309. https://doi.org/10.1007/s11604-011-0047-2

27. Feuerlein S, Pauls S, Juchems MS, et al (2009) Pitfalls in Abdominal Diffusion-Weighted Imaging: How Predictive is Restricted Water Diffusion for Malignancy. American Journal of Roentgenology 193:1070–1076. https://doi.org/10.2214/AJR.08.2093

28. Kyriazi S, Collins DJ, Messiou C, et al (2011) Metastatic Ovarian and Primary Peritoneal Cancer: Assessing Chemotherapy Response with Diffusion-weighted MR Imaging–Value of Histogram Analysis of Apparent Diffusion Coefficients. Radiology 261:182–192. https://doi.org/10.1148/radiol.11110577

29. Mori N, Ota H, Mugikura S, et al (2014) Luminal-Type Breast Cancer: Correlation of Apparent Diffusion Coefficients with the Ki-67 Labeling Index. Radiology 274:66–73. https://doi.org/10.1148/radiol.14140283

30. Kim HJ, Kim YK, Jeong WK, et al (2015) Pancreatic duct "Icicle sign" on MRI for distinguishing autoimmune pancreatitis from pancreatic ductal adenocarcinoma in the proximal pancreas. Eur Radiol 25:1551–1560. https://doi.org/10.1007/s00330-014-3548-4

31. De Robertis R, Cardobi N, Ortolani S, et al (2019) Intravoxel incoherent motion diffusion-weighted MR imaging of solid pancreatic masses: reliability and usefulness for characterization. Abdom Radiol 44:131–139. https://doi.org/10.1007/s00261-018-1684-z

32. Kim B, Lee SS, Sung YS, et al (2017) Intravoxel incoherent motion diffusion-weighted imaging of the pancreas: Characterization of benign and malignant pancreatic pathologies: IVIM DWI of the Pancreas. J Magn Reson Imaging 45:260–269. https://doi.org/10.1002/jmri.25334

33. Okazaki K, Chari ST, Frulloni L, et al (2017) International consensus for the treatment of autoimmune pancreatitis. Pancreatology 17:1–6. https://doi.org/10.1016/j.pan.2016.12.003